Accurate Analytical Model for Hybrid Ambient Thermal and RF Energy Harvester

Xiaoqiang Gu, Lei Guo, Moussa Harouna, Simon Hemour, Ke Wu

Accurate Analytical Model for Hybrid Ambient Thermal and RF Energy Harvester

Xiaoqiang Gu[1], Lei Guo[1], Moussa Harouna[1], Simon Hemour[2], Ke Wu[1]
[1]Polytechnique Montreal, Canada
[2]University of Bordeaux, France
Email: xiaoqiang.gu@polymtl.ca

***Abstract*— An accurate analytical model for the efficiency prediction of a hybrid ambient thermal and RF energy harvester is proposed in this paper. The DC power provided by the Thermoelectric Generator (TEG) is directly influencing the operation of the RF rectification. The proposed analytical model can provide an accurately predicted efficiency performance within a low-power range (< -30 dBm), thanks to a precise separation of each harmonic and DC component generated by diode. This has been verified by comparing with results obtained by both ADS simulation and experiments. Moreover, such a hybrid ambient thermal and RF energy harvester shows an advantage over its hybrid mechanical and RF energy harvesting counterpart in terms of rectified DC output power in the low-power range of interest. This is mainly due to the instinct of DC output converted from thermal energy and its huge contribution.**

***Index Terms*—hybrid energy harvester, thermal energy harvester, low-power harvesting, thermoelectric generator**

I. Introduction

To meet different energy consumption requirements of sophisticated sensors, intensive hybrid energy harvesting research has emerged recently, including a combination of two or even more types of RF, mechanical, thermal and solar energy [1]. Among different hybrid energy harvesting cases, thermal and RF energy harvesting is a typical one. The output of a thermal energy harvesting is DC power, acting as a bias of diode to shift its operating point. Thus, the introduction of thermal energy harvesting into a classical RF energy harvesting topology can produce a substantial improvement of efficiency performance. This hybrid thermal and RF energy harvesting was first reported in [2]. Though it shows performance improvement compared with single RF energy harvesting case as expected, there is still no comprehensive analytical model revealing how such a hybrid harvesting works collaboratively to lift the harvester's total efficiency. Considering a real-world application situation, ambient RF power is normally around -30 dBm or less. In the scope of this work, the DC power converted from TEG is also assumed to be at a similar power level. In such a low-power scenario, a theoretical model to accurately predict total efficiency performance is reported in this work once given input RF power level and bias voltage. The importance of the DC bias obtained from thermal energy harvesting in a low-power range is clearly observed. By comparing with a hybrid mechanical and RF energy harvester, this hybrid thermal and RF energy harvester demonstrates an obvious superiority in terms of DC output power.

II. Analytical Model for Hybrid Ambient Thermal and RF Energy Harvesting

The schematic diagram of a classical single diode based rectifier collecting both thermal and RF energy simultaneously is depicted in Fig. 1. Source #1 is the RF source with its internal resistance marked as R01. The equivalent circuit of the TEG that consists of a DC source and a low-value resistance is labeled as source #2. Both sources are isolated from each other by DC block C1 and RF choke L2. The energies generated by the sources are combined and injected into the packaged Schottky diode. Lp and Cp are packaging parasitic inductance and capacitance, respectively. The capacitance inserted in parallel with load resistor Rl is employed to smooth out AC component across the load. The Shockley diode model is used in the analysis which contains nonlinear junction resistance Rj, nonlinear junction capacitance Cj and series resistance Rs.

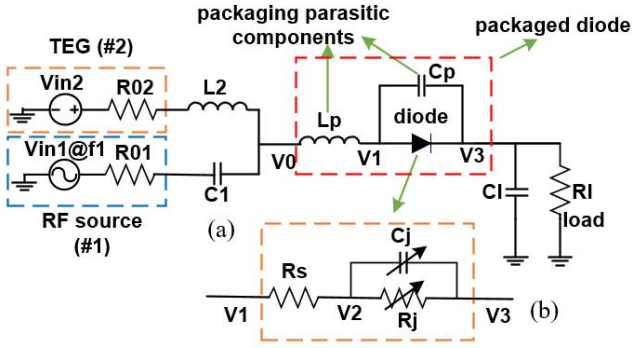

Fig. 1. (a) Diagram of a classical single diode based rectifier harvesting both thermal and RF energy. (b) Shockley diode model used in the analysis.

It is worth noting that a proper design of matching network with harmonic terminations can smooth out higher harmonics. Thus, maximum fundamental component is allowed to reach the rectifying diode [3]. Therefore, the matching network has been removed for simplification in Fig. 1, which enables us to clearly demonstrate the rectifying process of the hybrid thermal and RF harvester. The node voltages V0, V1, V2, and V3 identify corresponding voltage value at different points as shown in

the rectifying circuit diagram. Note that node voltages in both Fig. 1 (a) and (b) are kept consistent.

The RF source is assumed to generate a sinusoidal wave. When starting from the analysis of the voltage across the nonlinear junction resistance (between V2 and V3), one can reach:

$$\begin{aligned} \boldsymbol{V_{on}} &= \boldsymbol{V_{f_1}} + \boldsymbol{V_{dc\_in}} - \boldsymbol{V_{dc}} \\ &= v_{f_1} cos(2\pi f_1 t + \alpha_1) + v_{dc\_in} - v_{dc} \end{aligned} \quad (1)$$

It contains a fundamental component $\boldsymbol{V_{f_1}}$, a DC bias component $\boldsymbol{V_{dc\_in}}$ and a DC voltage $\boldsymbol{V_{dc}}$ generated by the diode itself. v_{f_1}, f_1 and α_1 are respectively the voltage magnitude, frequency and phase information of $\boldsymbol{V_{f_1}}$. And the magnitudes of $\boldsymbol{V_{dc\_in}}$ and $\boldsymbol{V_{dc}}$ are marked as v_{dc_in} and v_{dc}. $\boldsymbol{V_{dc}}$ pulls down the operating point of the diode to a lower voltage level, so it appears in (1) with a negative sign. v_{dc} can be calculated by DC current times total resistance in this circuit. The DC current i_{dc} only goes through TEG due to the existence of the DC block. Thus v_{dc} is:

$$v_{dc} = i_{dc} \cdot (R_l + R_s + R_{02}) \quad (2)$$

Based on the Shockley model, Schottky diode's I-V relationship is modeled by:

$$\begin{aligned} \boldsymbol{I_{diode}} &= I_s \cdot \left[e^{\frac{\boldsymbol{V_{on}}}{n \cdot Vt}} - 1 \right] \\ &= I_s \cdot [e^{\frac{v_{f_1} cos(2\pi f_1 t + \alpha_1) + v_{dc\_in} - v_{dc}}{n \cdot Vt}} - 1] \end{aligned} \quad (3)$$

in which Is and n are saturation current and ideality factor of the selected diode. $Vt = k \cdot T/q$ is the thermal voltage. k, T and q are the Boltzmann constant, operating temperature and electron charge, respectively. This exponential model can be considered accurate within this low-power range.

The next step is to separate diode current at different harmonics including the DC component. This has been done using Taylor series, but it may introduce some truncation errors which are more obvious at a higher power level [4]. With the help of Bessel function, this step can be done easily:

$$\begin{aligned} e^{\frac{v_{f_1} cos(2\pi f_1 t + \alpha_1)}{n \cdot Vt}} &= J_0\left(-i\frac{v_{f_1}}{n \cdot Vt}\right) + \\ & 2\sum_{k=1}^{\infty} i^k J_k\left(-i\frac{v_{f_1}}{n \cdot Vt}\right) cos[k \cdot (2\pi f_1 t + \alpha_1)] \end{aligned} \quad (4)$$

where $J_k(x)$ is the Bessel function of first kind of order k. So the DC current can be calculated by extracting the DC component in (4) and substituting it together with (2) into (3). By using the Lambert-W function, an explicit solution of i_{dc} is:

$$i_{dc} = I_s \cdot \left(\frac{W_0\left(G \cdot J_0\left(-i\frac{v_{f_1}}{n \cdot Vt}\right) \cdot e^{\frac{v_{dc\_in}}{n \cdot Vt}} \cdot e^G \right)}{G} - 1 \right) \quad (5)$$

where G is calculated by $(R_l + R_s + R_{02})/R_{j0}$. $R_{j0} = n \cdot Vt/I_s$ is the zero bias junction resistance. $W_0(x)$ in (5) is the 0th branch of the Lambert-W function. Therefore, the available DC power across the load can be expressed by:

$$P_{dc} = i_{dc}^2 \cdot R_l \quad (6)$$

In order to obtain the efficiency performance, both DC bias power converted from thermal energy and RF input power have to be determined. The DC bias power calculation is simple and can be expressed by $P_{dc\_in} = i_{dc} \cdot v_{dc\_in}$. Then, let us start calculating RF input power. Eq. (4) can be used to obtain the fundamental current as well:

$$\begin{aligned} \boldsymbol{I_{f_1}} &= i_{f_1} \cdot cos(2\pi f_1 t + \alpha_1) \\ &= I_s \cdot \left[2 \cdot i \cdot J_1\left(-i\frac{v_{f_1}}{n \cdot Vt}\right) \cdot e^{\frac{v_{dc\_in} - v_{dc}}{n \cdot Vt}} \right] \cdot cos(2\pi f_1 t + \alpha_1) \end{aligned} \quad (7)$$

Note that fundamental current going through the diode is assumed to be in-phase with the injecting voltage across the nonlinear junction. Within the diode, as shown in Fig. 1(b), by using the Kirchhoff Circuit Laws (KCL), the voltage at V1 can be calculated by:

$$\boldsymbol{V_{1f_1}} = \boldsymbol{V_{f_1}} + \left(\boldsymbol{I_{f_1}} + \boldsymbol{V_{f_1}} \cdot i\omega C_j\right) \cdot R_s \quad (8)$$

where $\omega = 2\pi f_1$ is the angular frequency. Applying KCL within the packaged diode, the voltage at V0 is expressed by:

$$\boldsymbol{V_{0f_1}} = \boldsymbol{V_{1f_1}} + \boldsymbol{I_{tf_1}} \cdot i\omega L_p \quad (9)$$

in which $\boldsymbol{I_{tf_1}}$ is the total current and calculated by:

$$\boldsymbol{I_{tf_1}} = \boldsymbol{V_{1f_1}} \cdot i\omega C_p + \boldsymbol{I_{f_1}} + \boldsymbol{V_{f_1}} \cdot i\omega C_j \quad (10)$$

Thus, the injecting RF power is able to be obtained now:

$$P_{f_1} = real\left(\frac{\boldsymbol{V_{0f_1}} \cdot \boldsymbol{I_{tf_1}^*}}{2}\right) \quad (11)$$

The total efficiency η of hybrid thermal and RF energy harvesting can be expressed by (12):

$$\eta = \frac{P_{dc}}{P_{dc\_in} + P_{f_1}} \times 100\% \quad (12)$$

III. Results and Discussion

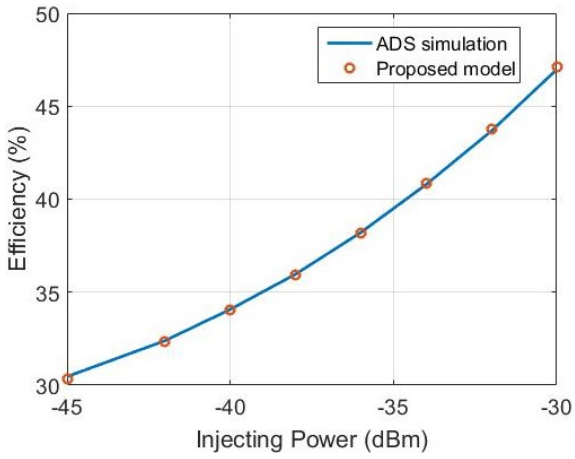

Fig. 2. Comparison of efficiency performance obtained from ADS simulation and proposed analytical model.

Firstly, a preliminary results comparison between ADS simulation and the proposed analytical model is conducted. The matching network loss is excluded here. The diode used is SMS7630-079LF, and the load is 5.4 kΩ. The RF power and DC bias power converted by TEG absorbed by diode are kept same and swept from -45 to -30 dBm. The efficiency performance comparison is shown in Fig. 2. The proposed analytical model clearly shows a good accuracy within this power range.

A collaborative measurement was done with RF power supplied by an external signal generator. The setup is shown in Fig. 3. Two multimeters are used for measuring the output voltages of TEG and harvester, respectively. To conduct a precise and reliable measurement of TEG, a thick foam with a rectangular hole is adopted as the heat isolation. A small aluminum block is inserted into the hole inside foam and the TEG is placed on it. Another bulky aluminum block is on the top of TEG, which firstly ensures a good contact between TEG and the small block, and secondly is the heat sink maintaining the top surface temperature at room temperature. A diagram presenting the setup details is provided on the upper left corner in Fig. 3. Note that a thermometer measuring the bottom surface temperature of TEG is adopted marked as a yellow bar in the diagram also.

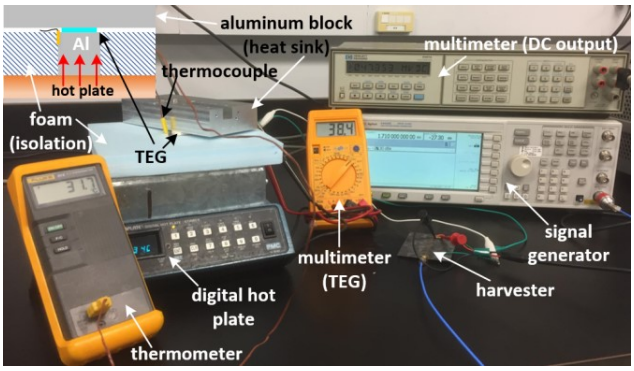

Fig. 3. Measurement setup of the hybrid harvester with a small diagram on the upper left corner showing the TEG measurement setup in detail.

During the cooperative measurement, the DC bias power and diode's RF injecting power were maintained the same and swept from -45 to -30 dBm. Through a preliminary ADS simulation, DC voltage for each bias power level was captured and then applied in the measurement. The temperature difference of TEG is defined by its top surface temperature (room temperature) and its bottom surface temperature (monitored by the thermometer). During the measurement, for example, a bias power of -30dBm requires about 78 mV which can be obtained by TEG with a temperature difference of 13.5 °C. This is roughly the difference between a human body temperature and a room temperature of 23.5 °C. Thus, the precise temperature control of the hot plate is used to adjust the output voltage of TEG. Measured DC output power of the hybrid thermal and RF power harvester versus injecting power is demonstrated in Fig. 4. It is clearly seen that the calculated results based on the proposed model match the measured ones well. Also, the DC output power rectified by a hybrid mechanical and RF power harvester is also presented for comparison [5]. The hybrid thermal and RF power harvester obviously shows a superior performance. Specifically, the output is 5.8 and 2.2 times larger than that of its mechanical counterpart at -40 and -30 dBm, respectively.

The measured results of separate thermal and RF power harvesting are also included in Fig. 4. If the hybrid thermal and RF power harvesting is considered as an organic combination of separate power harvesting cases, there is no doubt that thermal power harvesting is the dominant contributor. However, the output gap between these two separate power harvesting cases becomes close with an increasing injecting power. The output of single thermal energy harvesting is 23.4 times larger than that of single RF energy harvesting at -40 dBm and this number decreases to 4.4 at -30 dBm. This is mainly due to the rectifying efficiency of RF power harvesting improves dramatically with an increasing injecting power within this low-power range of interest. Since both mechanical and RF powers are both AC powers, this efficiency enhancement of AC power when injecting power becomes larger also explains the advantage of the hybrid thermal and RF power harvester diminishes over the hybrid mechanical and RF power harvester when power increases.

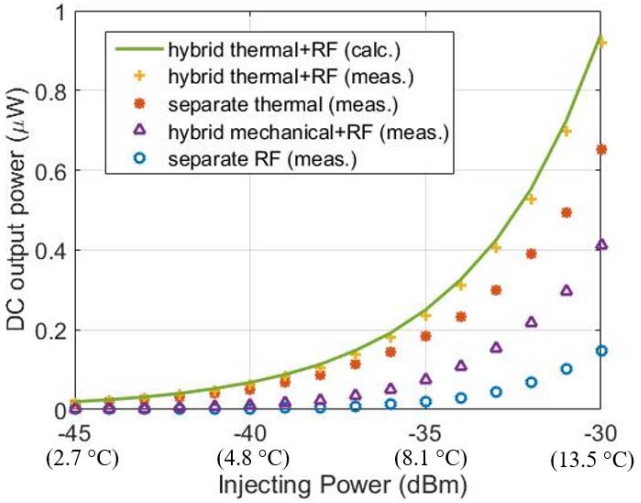

Fig. 4. Comparison of measured and calculated DC output power of the hybrid thermal and RF power harvester. The temperature differences for each bias power level are listed. The output power of a hybrid mechanical and RF power harvester plus separate power (thermal and RF power) harvesting are also presented. Matching network loss is excluded in the analysis.

IV. Conclusions

In this paper, an accurate analytical model for the efficiency prediction of a hybrid ambient thermal and RF power harvester is proposed and studied. The thermal source is simplified and considered as a DC power source in the analysis. Through comparison with both simulated and measured results, this model is verified to work well in a low-power range (< -30 dBm). In addition, this hybrid ambient thermal and RF power harvester can deliver much larger DC output power than its opponent (hybrid mechanical and RF power harvester). This is mainly due to the DC bias power offered by the thermal energy harvesting.

REFERENCE

[1] A. S. Weddell, *et al.*, "A survey of multi-source energy harvesting systems," in *Proc. DATE*, Mar. 18-22, 2013, pp. 905-908.

[2] M. Virili *et al.*, "Performance improvement of rectifiers for WPT exploiting thermal energy harvesting," *Wireless Power Transfer,* vol. 2, no. 1, pp. 22-31, 2015.

[3] F. Bolos, *et al.*, "RF Energy Harvesting From Multi-Tone and Digitally Modulated Signals," *IEEE Trans. Microw. Theory Techn.,* vol. 64, no. 6, pp. 1918-1927, 2016.

[4] C. H. Lorenz, *et al.*, "Hybrid power harvesting for increased power conversion efficiency," *IEEE Microw.Wireless Compon. Lett.,* vol. 25, no. 10, pp. 687-689, 2015.

[5] X. Gu, S. Hemour, and K. Wu, "Integrated cooperative radiofrequency (RF) and kinetic energy harvester," in *Proc. Wireless Power Transf. Conf.*, Taipei, Taiwan, May 2017, pp. 1-3.